and areas near and overlying the lesion site. Each patient was shown images of simple objects. Cortical stimulation, applied before the presentation of each image, was continued until there was a correct response or the next image was presented. Each pre-selected site was stimulated 3 to 4 times but never twice in succession. Sites where stimulation produced consistent speech arrest or anomia were considered essential language areas.

Case illustration

Case 1

This 49-year-old right-handed woman was in excellent health when she had her first generalized tonoclonic seizure. Preoperative MRI showed a round well-enhanced 2.5 cm lesion in the superior temporal gyrus. Intra-operative functional mapping of the essential speech cortex under awake surgery disclosed that the tumor was located just under the temporal language area. After exposing the posterior part of superior temporal plane by opening the Sylvian fissure, we performed intra-operative language mapping of the posterior part of the superior temporal plane. No language site was identified at that area. Unfortunately, we could not obtain an intra-operative pathological diagnosis, so we totally removed the lesion via a superior temporal plane cortical incision (Fig. 1). Postoperative histological diagnosis was primary CNS malignant lymphoma. This was treated with radio-chemotherapy as adjuvant therapy. Her postoperative SLTA score remained unchanged. She discharged from our hospital without any neurological deficits.

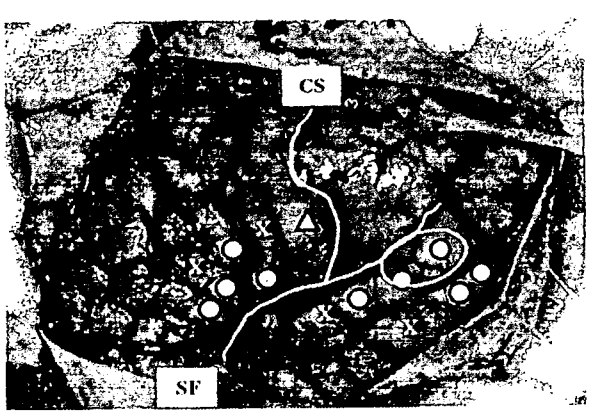

Fig. 1. *Case 1* – A 49-year-old woman with primary CNS malignant lymphoma. Intra-operative photograph of the brain map showing that the tumor is located under the Wernicke's area. O Speech arrest, Δ dysarthria, × no response, *CS* central sulcus, *SF* Sylvian fissure

Case 2

This 31-year-old woman was in excellent health when she sustained a simple head injury. CT study incidentally disclosed an anomaly. Preoperative MRI revealed a round, non-enhancing, 3 cm lesion in the inferior frontal gyrus. With the patient awake, intra-operative cortical functional mapping of the essential speech cortex was performed. A frontal language area was identified; the tumor was located under the tongue motor area. We exposed the frontal operculum by opening the Sylvian fissure and performed intra-operative language mapping. No language function was identified at the inner surface of the posterior part of the frontal operculum; the tumor was removed from the non language area (Fig. 2). The histological diagnosis was low-grade astrocytoma. Although she suffered transient dysarthria, she fully recovered within several days.

Case 3

This 52-year-old right-handed man was admitted to our hospital with aphasia and right-hand loss of power to grip. MRI showed a ring-like enhanced lesion in the frontal lobe. Intra-operative cortical language mapping failed to identify a frontal language area. His inferior frontal gyrus was swollen. We exposed the inner surface

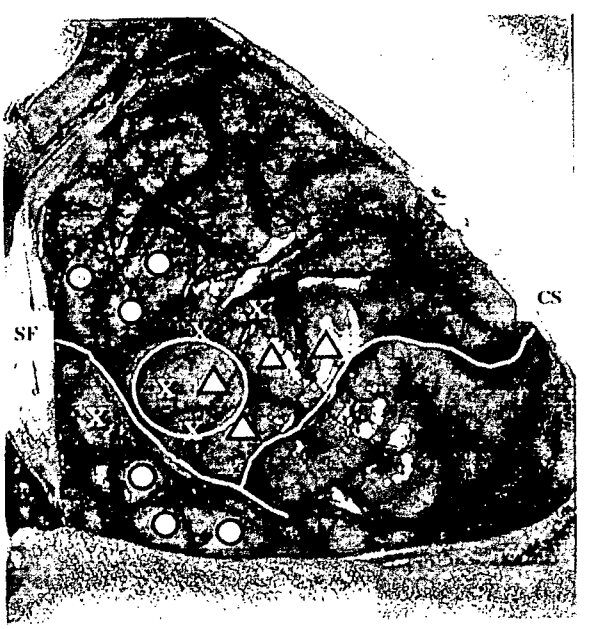

Fig. 2. *Case 2* – A 31-year-old woman with low-grade astrocytoma. Intra-operative photograph of the brain map showing that the tumor is located within the tongue motor area. O Speech arrest, Δ dysarthria, × no response, *CS* central sulcus, *SF* Sylvian fissure

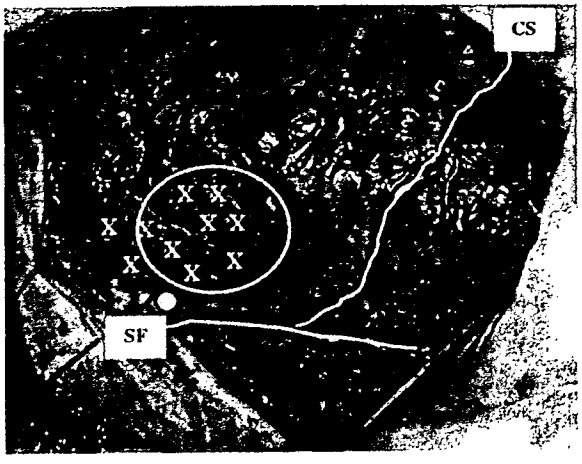

Fig. 3. *Case 3* – A 52-year-old man with frontal glioblastoma multiforme. Intra-operative photograph of the brain map showing that the Broca's area is located on the inside of the Sylvian fissure. O Speech arrest, Δ dysarthria, × no response, *CS* central sulcus, *SF* Sylvian fissure

of the frontal operculum by opening the Sylvian fissure and performed intra-operative language mapping again. The essential language area, located on the inner surface of the frontal operculum, was compressed by a tumor and shifted into the Sylvian fissure. We resected the tumor through the non-language cortex (Fig. 3). The language area was replaced to the surface of inferior frontal gyrus. The histological diagnosis was glioblastoma multiforme. His overall SLTA severity had worsened immediately after the operation, whereas it recovered and improved 3 months after surgery (Table 1b).

Case 4

This 55-year-old-man was admitted our hospital with transient epileptic motor aphasia. T1- and T2-weighed MRI showed a low- and a high-intensity lesion in the inferior frontal gyrus, respectively, which was not enhanced by gadolinium. His pre-operative interictal SLTA score was normal. During awake surgery, intra-operative functional mapping identified a frontal language area. The tumor was located under the language area. We opened the Sylvian fissure and performed intra-operative language mapping at the inside of the Sylvian fissure again. Because no essential language area was identified on the inner surface of the frontal operculum, we resected the tumor through this non-language area (Fig. 4). The histological diagnosis was oligodendroglioma. His postoperative SLTA score was also normal.

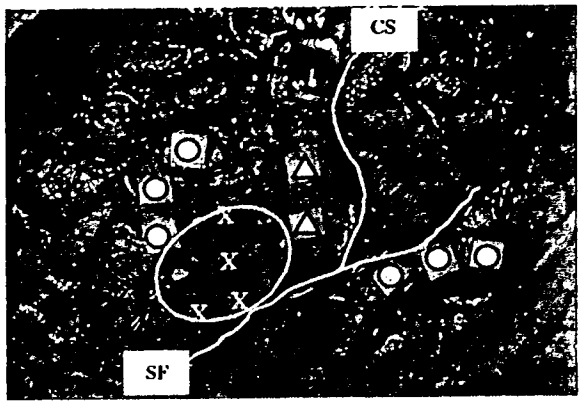

Fig. 4. *Case 4* – A 55-year-old man with oligodendroglioma. Intra-operative photograph of the brain map showing that the tumor is located under the Broca area. O Speech arrest, Δ dysarthria, × no response, *CS* central sulcus, *SF* Sylvian fissure

Case 5

This 44-year-old woman visited our hospital complaining of transient paraphasia. T2-weighted MRI showed a mixed-intensity lesion with a hypo-intense rim in the left superior temporal gyrus. Awake craniotomy was performed. Intra-operative functional mapping revealed that the tumor was located under Wernicke's area. We opened the Sylvian fissure and performed intra-operative language mapping of the planum temporale. No language function was identified at that area. We resected the tumor through the non-language area on the splanum temporale (Fig. 5). The diagnosis was cavernous angioma. Her postoperative SLTA score was normal.

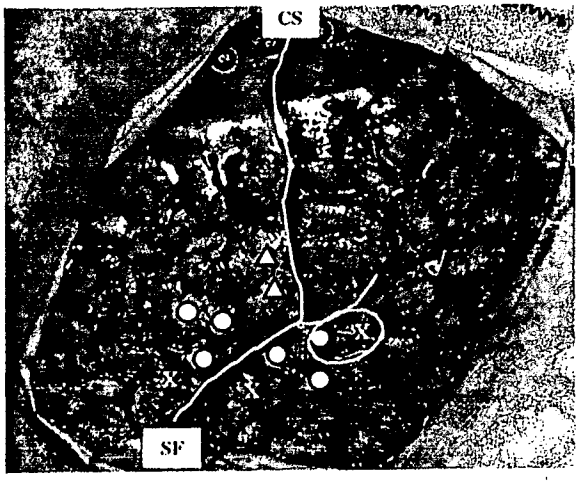

Fig. 5. *Case 5* – A 44-year-old woman with cavernous angioma. Intra-operative photograph of the brain map showing that the tumor is located under the Wernicke area. O Speech arrest, Δ dysarthria, × no response, *CS* central sulcus, *SF* Sylvian fissure

Summary of cases

Pre- and postoperative MRI of the 5 patients are shown in Fig. 6. Quality of resection was systemically evaluated using immediate (within 72 hr after the operation) post-operative MRI. We were able to remove all tumors totally without permanent new neurological deficits and without exacerbation of the patients' aphasia. Schematic drawings presented in Fig. 7 identify the localization of the 5 tumors and the language areas. Of the 5 patients, only case 3, a patient with

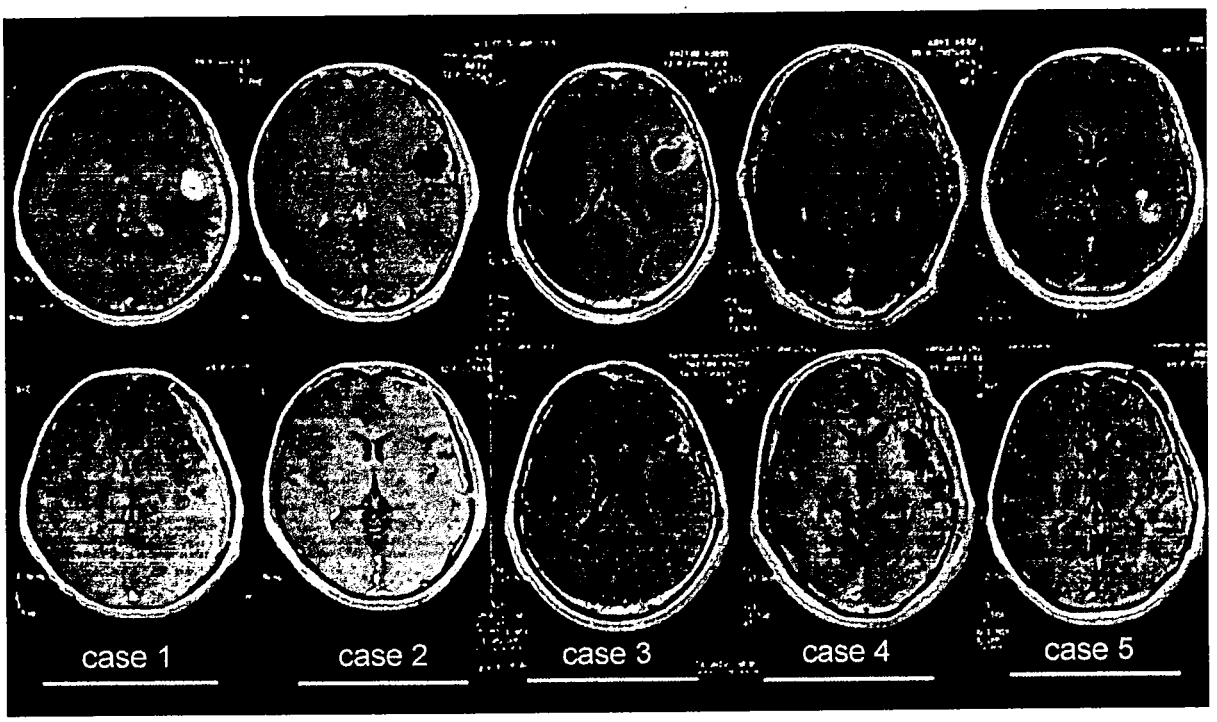

Fig. 6. Pre (*upper line*) – and post (*lower line*)-operative Gd-enhanced, T1-weighted magnetic resonance images obtained on the 5 patients. All tumors were removed almost totally

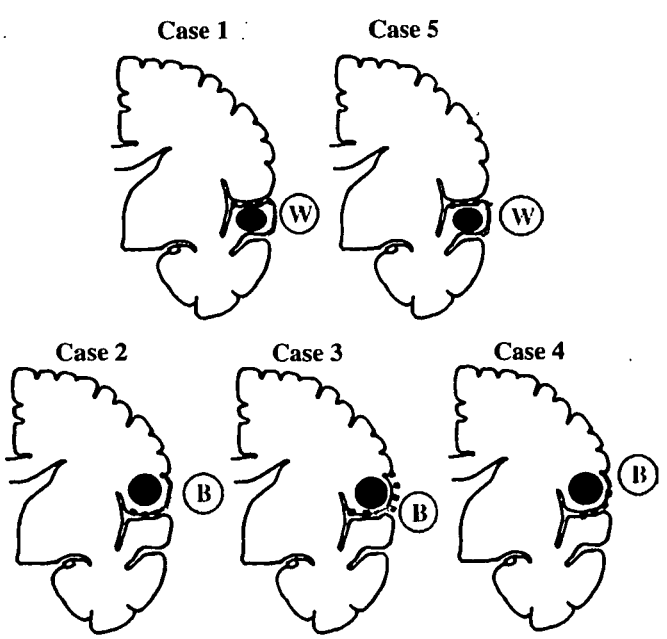

Fig. 7. Schematic drawing of the brain map of the 5 patients. *B* Broca's area, *W* Wernicke's area. The filled circles indicates the tumor. The dotted and gray lines encircle the functional- and non-functional areas, respectively

frontal glioblastoma manifested essential language function on the inner surface of the frontal or temporal operculum. This language area, located on the frontal operculum, appeared to be compressed and displaced by the tumor.

Discussion

Although functional mapping facilitates the planning of surgery in and around eloquent areas, the resection of tumors adjacent to language areas remains challenging. Ojemann and his associates reported that the essential language area localized to a focal areas of dominant hemisphere cortex of approximately 1 cm^2 [14, 15]. And the exact location of these sites in the left dominant hemisphere was found to vary substantially across the patient population. Haglund and colleagues reported that a margin of 7 to 10 mm around the language areas resulted in significantly fewer permanent postoperative linguistic deficits [9]. Recently, Duffau and colleagues noted no higher rate of definitive language worsening despite a resection coming in contact with the language sites (but higher rate of transient postoperative aphasia) [4]. Whittle IR *et al.* reported the incidence of iatrogenic dysphasia without intra-operative brain mapping is not dissimilar to that described after resection during use of awake craniotomy and intra-operative language testing [21]. They suggested that a large prospective study would be required to assess the usefulness of intra-operative language testing. Recently, Duffau H *et al.* reported that successful resection of a left insular cavernous angioma using intra-operative language mapping [5]. And Berger MS *et al.* mentioned that to maximize the extent of tumor resection while minimizing permanent language deficits, and recommended the using of cortical stimulation mapping [2]. Although this might be still controversial, we believe intra-operative language mapping is necessary to avoid surgical morbidity.

In this report, we took note that the language areas (Broca's and Wernicke's area) present at the perisylvian fissure. We posit that if there is non-essential language area on the inner surface of the Sylvian fissure, safe tumor resection may be possible even if the tumor is located under the language cortex. We operated on 3 patients with frontal gliomas without new neurological deficit except case 3 who experienced worsening of his aphasia transiently. But, his aphasia was improved 3 months after surgery.

The functional imaging studies allow detection of all the areas implicated in the realization of a task, but not the essential structures in these networks. There has been some work on the importance of the left frontal operculm for syntactic processing [6], and this region is activated during functional imaging studies of language. The functional imaging studies detected the distribution of 'essential' and 'participating' neuronal activity. But, the distribution of 'participating' neurons is substantially different to the focal, lateralized 'essential' sites identified by stimulation mapping for language. Noninvasive functional imaging modalities are an aid to the neurosurgeon, but the golden standard is still believed to be intra-operative monitoring. The evolution of better presurgical functional brain mapping techniques such as magnetic source imaging (MSI), fMRI, and probabilistic Diffuion Tensor imaging/fiber tracking methods will allow an estimation of the anatomical and functional cortex [7, 12]. These techniques may have the potential to promote functional neuronavigation as to an alternative to awake surgery.

The supratemporal plane of the temporal lobe in humans and subhuman primates contains the cortical representation of the primary and association auditory system and forms a part of Wernicke's area. However, the clinical presentation and treatment of patients with lesions in these areas have rarely been described. Silbergeld *et al.* who performed intra-operative cortical mapping during awake surgery on 2 patients subjected to resection of left-hemisphere Heschl gyrus gliomas, reported that neither patient manifested postoperative deficits [18]. Of 3 patients with non-dominant hemisphere Heschl's gyrus gliomas operated on by Russell and Golfinos [17], one presented with postoperative difficulty with music comprehension and production. In this report, we operated on 2 patients with left planum temporale tumors. We only examined language function intra-operatively. However, none of our 2 patients complained of auditory dysfunction and auditory change upon cortical stimulation. And we could remove the tumors without language dysfunction via non-functioning planum temporale cortex.

In our series, 4 of 5 patients had no essential language area on the inner surface of the operculum. Only one patient, a 52-year-old man with a frontal glioblastoma (Case 3) had language function on the inner surface of the frontal operculum. Duffau and colleagues reported 3 cases of inferior frontal gyrus (F3) glioma operated on without neurological deficits. They speculated that total F3 infiltration by glioma, thus a functional reorganization due to brain plasticity would explain the lack of deficit [3]. However, from intra-operative findings, after tumor removal, language cortex replaced on to the surface of the inferior frontal gyrus. We could not detect

essential language area on the medial area of the essential language area, and so we speculated his language area was compressed and displaced, rather than that there was reorganization of a new language area.

In conclusion, we posit that there is non-essential language area on the inner surface of the Sylvian fissure. While studies on larger patient populations are necessary, we can remove the perisylvian tumors through overlying non-language cortex. We propose our (opercular) approach may be useful in patients requiring the resection of perisylvian tumors.

Conclusions

Of 5 patients with tumors in the perisylvian cortex, only one, a patient with a frontal glioblastoma, manifested essential language function on the inner surface of the frontal operculum. In this exceptional case, the language cortex was compressed by the tumor and displaced to the inside of the Sylvian fissure. Based on the functional mapping data we obtained, we suggest that even tumors located in the subcortex of the language area may be resectable through the nonfunctioning opercular cortex without inducing postoperative language dysfunction.

References

1. Berger MS, Ojemann GA (1992) Intra-operative brain mapping techniques in neuro-oncology. Streotact Funct Neurosurg 58: 153–161
2. Berger MS, Ojemann GA (1999) Techniques for functional brain mapping during glioma surgery. In: Berger MS *et al* (eds) The Gliomas. W.B. Saunders Philadelphia, pp 421–435
3. Duffau H, Capelle L, Sichez N, Denvil D, Lopes M, Sichez JP, Bitar A, Fohanno D (2002) Intra-operative mapping of the subcortical language pathway using direct stimulations. Brain 125: 199–214
4. Duffau H, Capelle L, Denvil D, Siches N, Gatignol P, Taillandier L, Lopes M, Mitchell MC, Roche S, Muller JC, Bitar A, Sichez JP, van Effenterre R (2003) Usefulness of intra-operative electrical subcortical mapping during surgery for low-grade gliomas located within eloquent brain regions: functional results in a consecutive series of 103 patients. J Neurosurg 98: 764–778
5. Duffau H, Fontaine D (2005) Successful resection of a left insular cavernous angioma using neruonavigation and intra-operative language mapping. Acta Neurochir 147: 205–208
6. Friederici AD, Meyer M, Yves von Cramon D (2000) Auditory language conprehension: An event-related fMRI study on the processing of syntactic and lexical information. Brain and Language 74: 289–300
7. Ganslandt O, Buchfelder M, Hastreiter P, Grummich P, Falbusch R, Nimsky C (2004) Magnetic source imaging supports clinical decision making in glioma patients. Clin Nurol Neurosurg 107: 20–26
8. Hasegawa T, Kishi H, Shigeno K, Tanemura J, Kusunoki K, Kifune Y, Yoshida M (1984) A study on aphasia rating scale: a method for overall assessment of SLTA results. Higher Brain Function Res (Shitsugosyo-Kenkyu) 4: 638–646
9. Haglund MM, Berger MS, Shamseldin M, Lettich E, Ojemann GA (1994) Cortical localization of temporal lobe language sites in patients with gliomas. Neurosurg 34: 567–576
10. Kayama T, Sato S (2001) Definition of individual language related area by awake surgery. No To Shinkei 53: 151–160
11. Mimura M, Kato M, Sano Y, Kojima T, Naeser M, Kashima H (1998) Prospective and retrospective studies of recovery in aphasia. Changes in cerebral blood flow and language functions. Brain 121: 2083–2094
12. Nimsky C, Ganslandt O, Hastreiter P, Wang R, Benner T, Sorensen AG, Fahlbusch R (2005) Preoperative and intra-operative diffusion tensor imaging-based fiber tracking in glioma surgery. Neurosurg 56: 130–138
13. Ojemann SG, Berger MS, Lettich E, Ojemann GA (2003) Localization of language function in children: results of electrical stimulation mapping. J Neurosurg 98: 465–470
14. Ojemann GA (2003) The neurobiology of language and verbal memory: observations from awake neurosurgery. Int J Psychophysiol 48: 141–146
15. Ojemann G, Ojemann J, Lettich E, Berger M (1989) Cortical language localization in left, dominat hemispere. An electorical stimulation mapping investigation in 117 patients. J Neurosurg 71: 316–326
16. Roux FE, Boulanouar K, Lotterie JA, Mejdoubi M, LeSage JP, Berry I (2003) Language functional magnetic resonance imaging in preoperative assessment of language areas: correlation with direct cortical stimulation. Neurosurgery 52: 1335–1345
17. Russell SM, Golfinos JG (2003) Amusia following resection of a Heschl gyrus glioma. Case report. J Neurosurg 98: 1109–1112
18. Silbergeld DL (1997) Tumors of Heschl's gyrus: report of two cases. Neurosurgery 40: 389–392
19. Skirboll SS, Ojemann GA, Berger MS, Lettich E, Winn HR (1996) Functional cortex and subcortical white matter located within gliomas. Neurosurgery 38: 678–684
20. SLTA committee (1997) Standard Language Test of Aphasia: manual of directions. 2nd edn., Homeido, Tokyo
21. Whittle IR, Taylor PR (1998) Effects of resective surgery for left-sided intracranial tumours on language function: a prospective study. The Lancet 351: 1014–1018

Comment

This is an interesting study that emphasizes the value of intra-operative stimulation in awake patients during the resection of lesions adjacent to eloquent cortex. The authors hypothesize that even in the presence of lesions which seem unresectable because of location near Broca's or Wernicke's area, in selected cases a complete resection may be possible when the tumor is approached through a trans-opercular route of non-functional intrasylvian tissue on the inner' surface of the operculum.

In our opinion, however, awake craniotomy, while still regarded as the reference standard of surgery in eloquent cortex, should be considered an interim solution until the advent of better and more powerful functional imaging modalities that help us visualize functionally important brain tissue. We have experience with language MEG (magneto-encephalography) for over 5 years in about 120 cases operated upon for gliomas in the vicinity of Broca' and Wernicke's area with functional neuronavigation. From our experience we conclude that this may well be an alternative to intra-operative awake stimulation.

The evolution of better presurgical functional brain mapping techniques and probabilistic Diffusion Tensor Imaging/fibertracking methods will allow an estimation of the anatomical and functional cortex hitherto norknown. These techniques may have the potential to promote functional neuronavigation as to a true alternative to awake craniotomies.

More correlative studies will be warranted in the future to prove that these new techniques are as safe as the proven and tested method of intra-operative electrical stimulation.

References

1. Ganslandt O, Buchfelder M, Hastreiter P, Grummich P, Fahlbusch R, Nimsky C (2004) Magnetic source imaging supports clinical decision making in glioma patients. Clio Neurol Neurosurg 107: 20–26
2. Nimsky C, Ganslandt O, Hastreiter P, Wang R, Boher T, Sorensen AG, Fahlbusch R (2005) Preoperative and intra-operative diffusion tensor imaging-based fiber tracking in glioma surgery. Neurosurgery 56: 130–137

Rudolf Fahlbusch and *Oliver Ganslandt*
Erlangen

Correspondence: Takamasa Kayama, Department of Neurosurgery, Yamagata University, School of Medicine, 2-2-2 Iidanishi, Yamagata, #990-9585, Japan. e-mail: tkayama@med.id.yamagata-u.ac.jp

J Neurosurg 106:263–269, 2007

Ischemic complications associated with resection of opercular glioma

TOSHIHIRO KUMABE, M.D.,[1] SHUICHI HIGANO, M.D.,[2] SHOKI TAKAHASHI, M.D.,[2] AND TEIJI TOMINAGA, M.D.[1]

Departments of [1]Neurosurgery and [2]Diagnostic Radiology, Tohoku University Graduate School of Medicine, Sendai, Japan

Object. Opercular glioma inferolateral to the hand/digit sensorimotor area can be resected safely using a neuronavigation system and functional brain mapping techniques. However, the surgery can still sometimes cause postoperative ischemic complications, the character of which remains unclear. The authors of this study investigated the occurrence of infarction associated with resection of opercular glioma and the arterial supply to this region.

Methods. The study involved 11 consecutive patients with gliomas located in the opercular region around the orofacial primary motor and somatosensory cortices but not involving either the hand/digit area or the insula, who had been treated in their department after 1997. Both pre- and postoperative diffusion-weighted magnetic resonance (MR) imaging was performed in the nine consecutive patients after 1998 to detect ischemic complications. All patients underwent open surgery for maximum tumor resection. Postoperative MR imaging identified infarction beneath the resection cavity in all patients. Permanent motor deficits associated with infarction involving the descending motor pathway developed in two patients. Cadaveric angiography showed that the distributing arteries to the corona radiata were the long insular arteries and/or medullary arteries from the opercular and cortical segments of the middle cerebral artery.

Conclusions. Subcortical resection around the upper limiting sulcus of the posterior region of the insula and wide resection in the anteroposterior and cephalocaudal directions of the opercular region were considered to be risk factors of the critical infarction. Surgeons should be aware that resection of opercular glioma can disrupt the blood supply of the corona radiata, and carries the risk of permanent motor deficits.

KEY WORDS • **infarction** • **complication** • **glioma** • **descending motor pathway** • **operculum** • **diffusion-weighted imaging**

PRECISE localization of a glioma in the frontoparietal opercular region inferolateral to the hand/digit sensorimotor area is now possible using various methods including functional brain mapping techniques, neuronavigation systems, intraoperative MR imaging, and photodynamic diagnosis using various photosensitizers. Therefore, gliomas in this location, even in the dominant hemisphere, can be totally resected without causing permanent neurological deficits.[5,9,11,12] During such procedures, surgical techniques for opercular glioma have concentrated on the identification and preservation of the cortical and subcortical functions.[5,11,12] However, little is known about the ischemic complications that can occur after the resection of an opercular glioma.

Diffusion-weighted MR imaging, which reflects the degree of water diffusion in vivo, is an invaluable tool for the diagnosis of acute stroke and other types of brain injury.[14] Several potential applications of DW MR imaging in patients with gliomas have been recently investigated, mainly for the evaluation of tumor cellularity.[7,8,16,21] Recently, postoperative DW MR imaging has been proposed as a routine study to identify ischemic complications after resection of the glioma.[15] Diffusion-weighted MR imaging detected abnormalities after resection in approximately two thirds of newly diagnosed gliomas. At our institution, postoperative MR imaging including DW imaging has been performed for nearly 10 years as one of the examinations used to determine the postoperative state of patients after tumor removal and has disclosed evidence of postoperative ischemic complications.

In the present study we investigated the postoperative ischemic complications and DW MR imaging findings in 11 patients with pure opercular gliomas surgically treated during the past 9 years. Microangiography studies of cadavers were also analyzed to identify the blood supply for the corona radiata. Finally, referring to the results of the microangiographic analysis, we tried to determine the risk factors for critical infarction at the corona radiata that were likely to result in permanent motor deficits.

Abbreviations used in this paper: DW = diffusion-weighted; GBM = glioblastoma multiforme; MCA = middle cerebral artery; MR = magnetic resonance.

TABLE 1

*Summary of characteristics in 11 cases of opercular glioma**

Case No.	Age (yrs), Sex	Diagnosis	WHO Grade	Tumor Location	Dominant Hemisphere	Presenting Symptoms	Date of Surgery	State of Anesthesia
1	26, M	A	II	rt face motor area	no	lt facial seizure followed by generalized convulsion	1/23/97	awake
2	31, M	AA	III	lt face/tongue motor area	yes	generalized convulsion	9/11/97	awake
3	68, M	AA	III	rt tongue sensorimotor area	no	lt facial seizure	1/27/98	awake
4	3, M	DNET	I	rt face motor area	no	lt facial seizure	12/16/99	general
5	38, M	AA	III	lt face motor area	yes	lt facial seizure	2/28/00	general
6	69, F	GBM	IV	rt face/tongue sensorimotor area	no	lt facial seizure followed by lt hemiconvulsion	1/24/02	general
7	49, M	OA	II	rt tongue sensorimotor area	no	incidental	2/5/02	general
8	21, M	A	II	lt tongue sensorimotor area	no	rt facial seizure followed by generalized convulsion	4/11/02	general
9	38, M	AA	III	rt face motor area	no	lt facial seizure	7/22/02	general
10	34, F	O	II	lt face/tongue motor area	yes	rt facial seizure	4/28/03	awake
11	23, M	AA	III	lt face motor area	yes	loss of consciousness	6/9/05	awake

* A = astrocytoma; AA = anaplastic astrocytoma; DCS = direct cortical stimulation; DNET = dysembryoplastic neuroepithelial tumor; KPS = Karnofsky Performance Scale; O = oligodendroglioma; OA = oligoastrocytoma; SCS = subcortical stimulation; US = ultrasonography; WHO = World Health Organization.

Clinical Material and Methods

Patient Population and Tumor Characteristics

This study included 11 consecutive patients, nine males and two females with ages from 3 to 69 years (mean 36.4 ± 19.8 years). Each patient harbored a newly diagnosed glioma located at the opercular region around the orofacial primary motor and somatosensory cortices but not involving either the hand/digit area or the insula and treated in our department after 1997. The tumors included one dysembryoplastic neuroepithelial tumor, two astrocytomas, one oligoastrocytoma, one oligodendroglioma, five anaplastic astrocytomas, and one GBM. Patient characteristics are summarized in Table 1. Informed consent for this study was obtained from all the patients, and institutional review board approval was waived because of the retrospective nature of the study.

Surgical Procedure and Intraoperative Neurophysiological Monitoring

All patients underwent open surgery for maximum tumor resection. Cortical mapping was performed in eight patients, using electric stimuli of 3 to 12 mA to identify the sensorimotor and language cortices, according to a method described previously.[1-4] Five patients were treated while in an awake condition. Primary speech cortex was identified based on speech arrest or hesitation due to stimulation during counting or object naming by the patient. A frameless stereotactic navigation device (ISG Viewing Wand, ISG Technologies; ViewScope, Elekta IGS; or Vector Vision, BrainLAB) was used in all nine cases after 1998; ultrasonography was used in the initial two cases.

Tumor resection was performed using an Ultrasonic Surgical Aspirator (Sonopet, Miwatec Co., Ltd.). All of the opercular arteries were carefully dissected and preserved. If the tumor infiltrated down to the sylvian fissure, thorough dissection of the affected sylvian fissure was initially performed to identify and preserve the insular and opercular segments of the MCAs.

Only the minimum amount of Surgicel (Ethicon, Inc.) was routinely used for hemostasis. Dexamethasone (4 mg) was given every 6 hours with varied tapering schedules, and the administration of anticonvulsants (typically phenytoin and/or zonisamide) and antibiotics was begun or continued in patients during the immediate postoperative period.

Neuroimaging Studies

All patients underwent preoperative, postoperative, and subsequent follow-up MR imaging at our department. Postoperative imaging was performed within 72 hours of surgery. Data from pre- and postoperative DW MR imaging were available for the nine consecutive patients treated after 1998.

For MR imaging, we used a 1.5-tesla system (Signa Horizon LX CV/i, GE Medical Systems) with a conventional quadrature head coil. We obtained T_1-weighted images before and after Gd administration, T_2-weighted images, and DW images during the same imaging session without repositioning the patient's head. Axial DW images were obtained using fat-suppressed spin echo–echo planar imaging (TR 5000 msec, TE 72 msec, number of excitations 2, slice thickness 6 mm, gap 2 mm, matrix 128 × 128, and field of view 23 × 23 cm) with three orthogonal directional motion-probing gradients (b = 1000 seconds/mm^2), followed by automatic generation of isotropic DW images. To evaluate the

TABLE 1
(continued)

Stimulation	Navigation System	Extent of Resection	DW Image	Immediate Postop Outcome	Long-Term Deficit	Follow Up (3/26/06)
DCS	US	total	not examined	lt facial palsy	none	no recurrence, KPS 100
DCS	US	total	not examined	rt facial palsy, dysarthria	slight dysarthria	no recurrence, KPS 90
DCS	viewing wand	total	infarction beneath resection cavity	lt hemiparesis	lt fine movement disorder	dead 5/14/99 (dissemination)
none	ViewScope	total	infarction beneath resection cavity	lt hemiparesis	none	no recurrence, KPS 100
DCS & SCS	ViewScope	total	infarction beneath resection cavity	rt facial palsy, dysarthria	slight dysarthria	no recurrence, KPS 90
DCS & SCS	ViewScope	subtotal	infarction beneath resection cavity	lt hemiparesis	lt hemiparesis	dead 4/28/04 (local recurrence & dissemination)
none	ViewScope	total	infarction beneath resection cavity	lt facial palsy	none	no recurrence, KPS 100
none	ViewScope	total	infarction beneath resection cavity	none	none	no recurrence, KPS 100
DCS & SCS	ViewScope	total	infarction beneath resection cavity	none	none	no recurrence, KPS 100
DCS & SCS	ViewScope	subtotal	infarction beneath resection cavity	rt facial palsy, dysarthria	dysarthria	no recurrence, KPS 90
DCS & SCS	Vector Vision	subtotal	infarction beneath resection cavity	rt fine movement disorder, dysarthria	none	no recurrence, KPS 100

spatial relationship between the postoperative ischemic lesion and the pyramidal tract, coronal DW images were also obtained using similar conditions, but the motion-probing gradient was applied in only the anteroposterior direction. The pyramidal tracts, which run in the cephalocaudal direction, were delineated as slightly hyperintense to adjacent brain parenchyma in these coronal images.

The extent of the resection was evaluated according to MR images obtained within 72 hours of surgery. If the tumor had been enhanced on the preoperative MR images, its gross-total resection was defined as no residual enhanced tumor, its subtotal resection as more than 75% removal, and its partial resection as less than 75% removal. If the tumor had not been enhanced on the preoperative MR images, resection was evaluated based on the presence of residual high-intensity lesion on the T_2-weighted MR images.

Postoperative Neurological Outcomes

The postoperative neurological outcome was recorded and confirmed by retrospective review of all hospital records and physician notes. Immediate postoperative neurological function was determined during the first 7 days after surgery, and long-term function was determined between 3 and 6 months after surgery.

Microangiographic Analysis of Vascular Supply to the Corona Radiata

Coronal and axial microangiograms of five cadaveric brains without gross brain pathological features, which were part of a microangiographic study on the distribution of the basal perforating arteries that had been conducted by one of the authors (S.T.) in 1985,[17,18] were reanalyzed to examine pial cortical arteries in and around the insuloopercular region and to identify the blood supply to the corona radiata.

Results

Extent of Resection

Table 1 outlines the extent of resection in each case, as determined by quantitative volumetric analysis using postoperative MR imaging. Gross-total resection of the lesions was accomplished in eight patients (Cases 1–5 and 7–9). Subtotal resection was achieved in three patients (Cases 6, 10, and 11).

Postoperative MR Imaging and Neurological Outcomes

Postoperative DW MR images showed markedly hyperintense areas representing restricted diffusion in all nine patients treated after 1998. These lesions were all contiguous with the resection cavity. The size of the lesions beneath the resection cavity varied from case to case. All lesions appeared as high-intensity areas on T_2-weighted MR images. Similar high-intensity lesions were also depicted on postoperative T_2-weighted images in the two initial patients without DW imaging data.

Details on postoperative neurological deficits are shown in Table 1. Eight patients, all of whom had undergone relatively small areas of resection mostly located in the face motor area, did not suffer impairment of long-tract function after surgery; three patients (Cases 3, 4, and 6) did have impaired long-tract function immediately after surgery. The lesions with restricted diffusion involved the descending motor pathway in these three patients. Tumor was located in the orofacial sensorimotor area in two of these patients

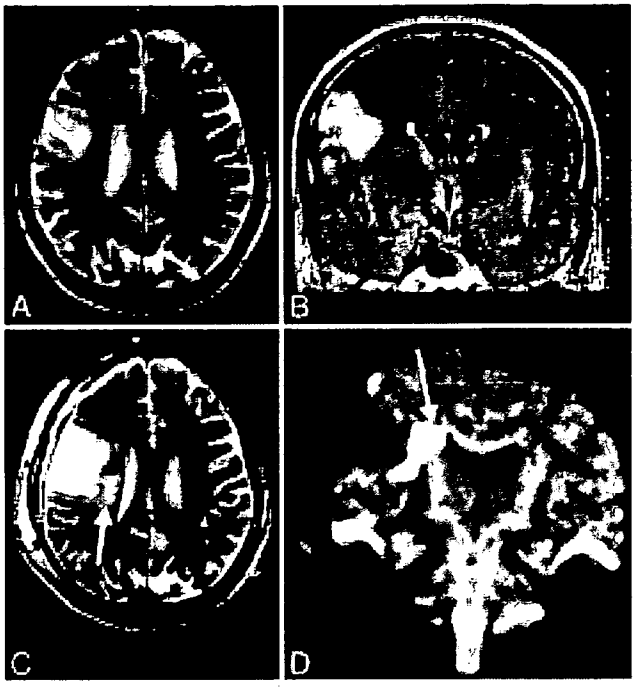

FIG. 1. Case 3. Images obtained in a 68-year-old man with an anaplastic astrocytoma in the right tongue sensorimotor area. Preoperative axial T_2-weighted (A) and coronal fluid-attenuated inversion-recovery (B) MR images revealing a high-intensity mass in the right frontoparietal opercular region. Postoperative axial T_2-weighted (C) and coronal DW (D) MR images showing total removal of the tumor and a new high-intensity lesion *(arrows)* beneath the resection cavity. The lesion extends to the region of the corona radiata, probably involving the corticospinal tract. This tract appears as a bandlike area of slightly high intensity on the coronal DW image with the motion-probing gradient applied only in the anteroposterior direction.

(Cases 3 and 6). A relatively small resection in these two patients was performed around the white matter above the upper limiting sulcus of the posterior region of the insula, and wide resection was undertaken in the anteroposterior and cephalocaudal directions of the opercular region (Figs. 1–4).

Microangiographic Analysis of Vascular Supply to the Corona Radiata

Coronal microangiography of the cadavers showed that the corona radiata is constantly supplied by the lateral striate arteries, the long insular arteries originating from insular portions of the MCA, and the medullary arteries from the opercular and cortical portions of the MCA (Fig. 5). Surgical removal for opercular glioma, even if not involving the insula, could compromise the latter two fine arteries, resulting in cerebral infarction at the corona radiata.

Illustrative Cases

Case 3

History and Examination. This 68-year-old man presented with an anaplastic astrocytoma manifesting as left facial seizures. Results of T_2-weighted MR imaging demonstrated a hyperintense lesion in the right opercular portions of the inferior frontal, precentral, and postcentral gyri inferolateral to the precentral knob, not involving the insula (Fig. 1A). Administration of a contrast medium caused no enhancement. Neurological and neuropsychological examination revealed no abnormality.

Operation. A right frontoparietotemporal craniotomy was performed with the patient in an awake condition. Direct cortical stimulation identified the face motor area and the primary sensory sites of the tongue and face. The sylvian fissure was thoroughly dissected toward the distal end, and the insular surface was exposed under the operating microscope. The precentral and central arteries were separated from the tumor and preserved. The lesion was totally removed up to the face motor area and toward the deepest portion using the upper limiting sulcus as the anatomical landmark and the ISG Viewing Wand (Fig. 2).

Postoperative Course. Almost complete left hemiparesis was observed postoperatively. Magnetic resonance images showed that the entire lesion had been resected but revealed an ischemic area beneath the resection cavity involving the descending motor pathway (Fig. 1B). As adjuvant therapy, the patient received 72 Gy hyperfractionated radiation to the extended local field. His left hemiparesis resolved except

FIG. 2. Case 3. Intraoperative photographs obtained before *(left)* and after *(right)* tumor resection. *Left:* Note the results of functional brain mapping: 1, face motor; 2, tongue sensory; and 3, face sensory. The outline indicates the location of the tumor; the *arrows* represent the central sulcus. *Right:* Note preservation of the precentral (4) and central (5) arteries.

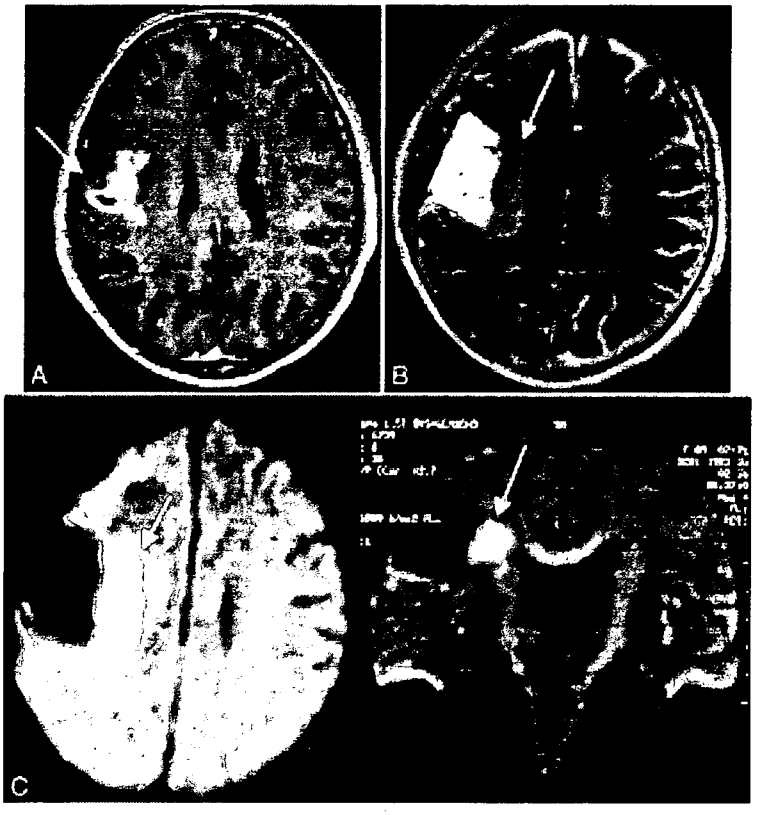

FIG. 3. Case 6. Images obtained in a 69-year-old woman with a right frontoparietal GBM. A: Preoperative axial Gd-enhanced T_1-weighted MR image demonstrating an irregularly enhanced mass lesion in the opercular region around the central sulcus *(arrow)*. B: Postoperative axial T_2-weighted MR image depicting total removal of the tumor and a new lesion of high intensity *(arrow)* beneath the resection cavity. C: Postoperative axial *(left)* and coronal *(right)* DW MR images revealing the new lesion *(arrows)* beneath the resection cavity with reduced diffusion probably involving the corticospinal tract.

for impaired fine movement of the left finger. He was discharged home and able to ambulate 2 months postsurgery.

Case 6

History and Examination. This 69-year-old woman presented with a GBM manifesting as left facial seizures followed by left hemiconvulsion. Preoperative T_1-weighted MR images with contrast medium exhibited an enhanced mass in the right opercular portions of the inferior frontal, precentral, and postcentral gyri inferolateral to the precentral knob, not involving the insula (Fig. 3A). Neurological and neuropsychological examination revealed no abnormality.

Operation. A right frontoparietotemporal craniotomy was performed with the patient in a state of general anesthesia. Direct cortical stimulation identified the hand/digit motor area. The sylvian fissure was thoroughly dissected toward the distal end, and the insular surface was exposed under the operating microscope. The precentral, central, and anterior parietal arteries were separated from the tumor and preserved. The lower portion of the lesion was resected toward the deepest portion by using the upper limiting sulcus as the anatomical landmark and the ViewScope. The tumor was removed in a stepwise manner while monitoring the muscle contraction by direct cortical stimulation to the hand/digit motor area (Fig. 4). The positive cortical response gradually became duller at the end of the surgery.

Postoperative Course. Almost complete left hemiparesis was observed postoperatively. Magnetic resonance images obtained after surgery showed that most of the enhanced lesion had been resected, but an ischemic area was found beneath the resection cavity involving the descending motor pathway (Fig. 3B and C). The patient's left hemiparesis did not resolve.

Discussion

Surgical removal of glioma in the opercular region presents many challenges. In 1991, LeRoux et al.[11] first reported that gliomas involving the nondominant face motor cortex can be safely removed using brain mapping techniques to localize the rolandic cortex and avoid resection of the hand motor cortex and descending subcortical motor pathways. However, resection of the face motor cortex in the dominant hemisphere was not recommended because language localization in the cortical zones is contiguous with this region. In 1995, Ebeling and Kothbauer[5] supposed that radical tumor resection of a purely opercular glioma, not including the insula, in the dominant hemisphere can be

FIG. 4. Case 6. Intraoperative photographs obtained before *(left)* and after *(right)* tumor resection. *Left:* Note the results of functional brain mapping: 1 and 2, hand/digit motor. The *outline* indicates the tumor location; the *arrows* represent the central sulcus. *Right:* Note preservation of the precentral (3), central (4), and anterior parietal (5) arteries.

achieved without significant lasting morbidity. However, only biopsy was recommended for large dominant insular or opercular–insular tumors, because the lenticulostriate arteries hinder total resection and no clear border toward the internal capsule can be found. In 2004, Peraud et al.[12] reported the surgical results of 14 cases of opercular gliomas, stressing the importance of intraoperative neuromonitoring as an aid to surgery in the dominant opercular region. The severity and duration of postoperative deficits was well correlated with the distance from the resection margin to the next positive stimulation point(s), and a distance of more than 5 mm was found to avoid major impairments. Clearly, intraoperative functional brain mapping techniques can help preserve cortical and subcortical functions. However, vascular damage during resection of opercular glioma remains less well understood.

Recently, restricted diffusion abnormalities were found adjacent to the resection cavity on immediately postoperative images in 64% of cases.[15] Both cortical and subcortical lesions with restricted diffusion were observed after surgery. In the present study, postoperative MR images including DW images disclosed infarcted lesions in all patients, and these lesions unexpectedly extended to the descending motor pathway in the corona radiata in three patients, which could have resulted in the impairment of long-tract function. These infarcted lesions were probably caused by disruption of the blood supply during the surgical procedures.

Microangiographic analysis in this study revealed that the corona radiata is supplied by the lateral striate arteries, long insular arteries, and medullary arteries from the opercular and cortical segments of the MCA passing over the frontoparietal operculum. According to the study data collected by Ture et al.,[20] approximately 85 to 90% of insular arteries are short and supply the insular cortex and extreme capsule, 10% are medium length and supply the claustrum and external capsule, and 3 to 5% are long and extend as far

FIG. 5. Coronal *(left)* and axial *(right)* microangiograms of a cadaveric brain slice through the interventricular foramina. Both long insular arteries *(arrows)* arising from the insular portions of the MCA and the medullary arteries *(arrowhead)* from the opercular and cortical portions of the MCA course toward the ventricular wall and supply the region of the corona radiata.

as the corona radiata. Interruption of blood flow to these long insular arteries during the resection of intrinsic insular tumor may result in hemiparesis; thus, these arteries should be preserved to prevent infarction of the corona radiata.[6,10,19,20]

Data in the present study demonstrated that, in addition to the long insular arteries, the long medullary arteries from the opercular and cortical segments of the MCA passing over the frontoparietal operculum contribute to the arterial supply to the corona radiata. Although the vascular supply can show individual variations, these long medullary arteries can be impaired during the resection of a pure opercular glioma. Adequate collateral blood supply would not be expected[13] because intraparenchymal arterioles such as the lateral striate arteries, long insular arteries, and long medullary arteries are all end arteries without substantial anastomoses with other arteries except in pathological cases like moyamoya disease. If the impaired arteries supply most of the descending motor pathway, resection of opercular glioma is likely to result in hemiparesis.

The long insular arteries are mostly located in the posterior region of the insula,[20] most commonly on the posterior half of the central insular sulcus and on the long gyri.[19] Thus, subcortical resection around the upper limiting sulcus of the posterior region of the insula carries a higher risk of sacrifice of the long insular arteries, which may lead to extensive corona radiata infarction, and ultimately critical damage to the descending motor pathway. Similarly, a wide resection in the anteroposterior and cephalocaudal directions of the opercular region could damage a large number of medullary arteries from the opercular and cortical segments of the MCA over the frontoparietal operculum. In our experience, these two maneuvers appeared to be risk factors for critical infarction in the corona radiata after resection of an opercular glioma. However, reliable methods for avoiding damage to the long insular and medullary arteries are not available. Limited resection of the operculum as well as sparing of the posterior region of the insula may be the only measures presently available to avoid injury to a large number of long insular arteries and long medullary arteries. The development of new surgical devices to remove an opercular glioma with preservation of thin blood vessels like these arteries is to be expected in the future.

Conclusions

In the present study we found that ischemic complications occurring beneath the resection cavity including the pyramidal tract within the corona radiata are caused by damage to the distributing arteries—in particular, the long insular arteries and/or medullary arteries from the opercular and cortical segments of the MCA passing over the frontoparietal operculum—after resection of glioma in the frontoparietal opercular region inferolateral to the hand/digit sensorimotor area. Surgeons should be aware of the risk of ischemic complications during resection of opercular glioma and the possibility of permanent motor deficits.

References

1. Berger MS: Malignant astrocytomas: surgical aspects. **Semin Oncol 21:**172–185, 1994
2. Berger MS, Deliganis AV, Dobbins J, Keles GE: The effect of extent of resection on recurrence in patients with low grade cerebral hemisphere gliomas. **Cancer 74:**1784–1791, 1994
3. Berger MS, Kincaid J, Ojemann GA, Lettich E: Brain mapping techniques to maximize resection, safety, and seizure control in children with brain tumors. **Neurosurgery 25:**786–792, 1989
4. Berger MS, Ojemann GA, Lettich E: Neurophysiological monitoring during astrocytoma surgery. **Neurosurg Clin N Am 1:** 65–80, 1990
5. Ebeling U, Kothbauer K: Circumscribed low grade astrocytomas in the dominant opercular and insular region: a pilot study. **Acta Neurochir 132:**66–74, 1995
6. Hentschel SJ, Lang FF: Surgical resection of intrinsic insular tumors. **Neurosurgery 57 (1 Suppl):**176–183, 2005
7. Higano S, Yun X, Kumabe T, Watanabe M, Mugikura S, Umetsu A, et al: Malignant astrocytic tumors: clinical importance of apparent diffusion coefficient in prediction of grade and prognosis. **Radiology 241:**839–846, 2006
8. Kitis O, Altay H, Calli C, Yunten N, Akalin T, Yurtseven T: Minimum apparent diffusion coefficients in the evaluation of brain tumors. **Eur J Radiol 55:**393–400, 2005
9. Kumabe T, Nakasato N, Suzuki K, Sato K, Sonoda Y, Kawagishi J, et al: Two-staged resection of a left frontal astrocytoma involving the operculum and insula using intraoperative neurophysiological monitoring—case report. **Neurol Med Chir 38:**503–507, 1998
10. Lang FF, Olansen NE, DeMonte F, Gokaslan ZL, Holland EC, Kalhorn C, et al: Surgical resection of intrinsic insular tumors: complication avoidance. **J Neurosurg 95:**638–650, 2001
11. LeRoux PD, Berger MS, Haglund MM, Pilcher WH, Ojemann GA: Resection of intrinsic tumors from nondominant face motor cortex using stimulation mapping: report of two cases. **Surg Neurol 36:**44–48, 1991
12. Peraud A, Ilmberger J, Reulen HJ: Surgical resection of gliomas WHO grade II and III located in the opercular region. **Acta Neurochir 146:**9–18, 2004
13. Phan TG, Donnan GA, Wright PM, Reutens DC: A digital map of middle cerebral artery infarcts associated with middle cerebral artery trunk and branch occlusion. **Stroke 36:**986–991, 2005
14. Schaefer PW, Grant PE, Gonzalez RG: Diffusion-weighted MR imaging of the brain. **Radiology 217:**331–345, 2000
15. Smith JS, Cha S, Mayo MC, McDermott MW, Parsa AT, Chang SM, et al: Serial diffusion-weighted magnetic resonance imaging in cases of glioma: distinguishing tumor recurrence from postresection injury. **J Neurosurg 103:**428–438, 2005
16. Sugahara T, Korogi Y, Kochi M, Ikushima I, Shigematu Y, Hirai T, et al: Usefulness of diffusion-weighted MRI with echo-planar technique in the evaluation of cellularity in gliomas. **J Magn Reson Imaging 9:**53–60, 1999
17. Takahashi S, Goto K, Fukasawa H, Kawata Y, Uemura K, Suzuki K: Computed tomography of cerebral infarction along the distribution of the basal perforating arteries. Part I: Striate arterial group. **Radiology 155:**107–118, 1985
18. Takahashi S, Goto K, Fukasawa H, Kawata Y, Uemura K, Yaguchi K: Computed tomography of cerebral infarction along the distribution of the basal perforating arteries. Part II: Thalamic arterial group. **Radiology 155:**119–130, 1985
19. Tanriover N, Rhoton AL Jr, Kawashima M, Ulm AJ, Yasuda A: Microsurgical anatomy of the insula and the sylvian fissure. **J Neurosurg 100:**891–922, 2004
20. Ture U, Yaşargil MG, Al-Mefty O, Yaşargil DC: Arteries of the insula. **J Neurosurg 92:**676–687, 2000
21. Zimmerman RD: Is there a role for diffusion-weighted imaging in patients with brain tumors or is the "bloom off the rose"? **AJNR 22:**1013–1014, 2001

Manuscript submitted March 26, 2006.
Accepted August 7, 2006.

Address reprint requests to: Toshihiro Kumabe, M.D., Department of Neurosurgery, Tohoku University Graduate School of Medicine, 1–1 Seiryo-machi, Aoba-ku, Sendai 980–8574, Japan. email: kuma@nsg.med.tohoku.ac.jp.

Neurol Med Chir (Tokyo) 47, 229~232, 2007

Complete Response to Temozolomide Treatment in an Elderly Patient With Recurrent Primary Central Nervous System Lymphoma

—Case Report—

Keishi MAKINO, Hideo NAKAMURA, Mareina KUDO, Hideo TAKESHIMA, and Jun-ichi KURATSU

Department of Neurosurgery, Kumamoto University Graduate School, Kumamoto, Kumamoto

Abstract

An 80-year-old woman presented with primary central nervous system (CNS) lymphoma manifesting as progressive disorientation and loss of activity. She received three cycles of high-dose methotrexate. The tumor shrank after two cycles and her mental status improved, but she suffered tumor recurrence. The second-line treatment consisted of four cycles of rituximab but the tumor enlarged. She was then treated with three cycles of temozolomide. Magnetic resonance imaging revealed no evidence of disease. Her mental status and performance status improved, and she suffered no toxicity. She is able to pursue her daily life without recurrence after 16 cycles of temozolomide. Temozolomide may be effective against relapsed primary CNS lymphoma without causing neurotoxicity in the elderly.

Key words: primary central nervous system lymphoma, temozolomide, elderly, recurrence, rituximab

Introduction

The introduction of high-dose methotrexate (MTX) treatment has resulted in markedly improved survival of patients with primary central nervous system (CNS) lymphoma.[6,8,20] After treatment with high-dose MTX, 50–65% of patients showed complete and 20–35% showed partial radiographic response.[2,5,10,17] However, 10–35% of patients have tumors which are refractory to the high-dose MTX regimen and up to 60% of complete responders manifest tumor recurrence during follow up.[22,24] Furthermore, over 90% of patients older than 60 years who were successfully treated with a combination of chemotherapy and whole-brain radiotherapy later developed treatment-related neurotoxicity characterized by dementia, gait abnormalities, and urinary incontinence.[1,2]

Temozolomide is an oral alkylating agent that spontaneously undergoes chemical conversion to the cytotoxic metabolite MTIC (5-(3 methyl-1-triazeno)immidazole-4-carboxamide) at physiological pH without metabolic conversion. This metabolite depletes the deoxyribonucleic acid (DNA)-repair enzyme O^6 methylguanine-DNA methyltransferase in various cell types. Alkylating agents are generally effective against non-Hodgkin's lymphoma, and temozolomide has good CNS penetration and a favorable toxicity profile.[12,25] Therefore, temozolomide may be useful in the treatment of primary CNS lymphoma.

We initially treated an 80-year-old woman with primary B-cell CNS lymphoma with high-dose MTX. However, complete response was not obtained after three cycles. Her advanced age and compromised mental status increased the risk of complications from whole-brain irradiation after high-dose MTX, so we administered three cycles of temozolomide as a third-line therapy after four cycles of rituximab. Magnetic resonance (MR) imaging revealed no evidence of disease. Her mental and performance status improved and there was no evidence of recurrence 16 months after temozolomide therapy.

Case Report

An 80-year-old woman had a 1-month history of

Received July 27, 2006; Accepted February 13, 2007

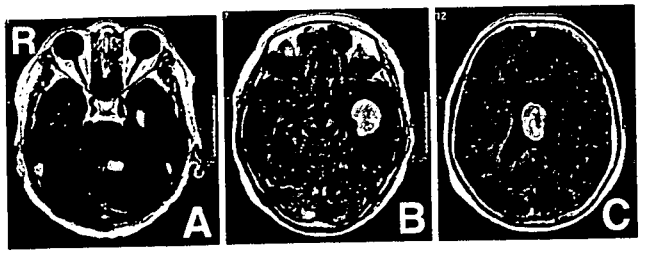

Fig. 1 T_1-weighted magnetic resonance images with contrast medium showing a diffusely enhanced lesion in the left temporal horn of the lateral ventricle (B), septum pellucidum (C), and periventricular area of the fourth ventricle (A).

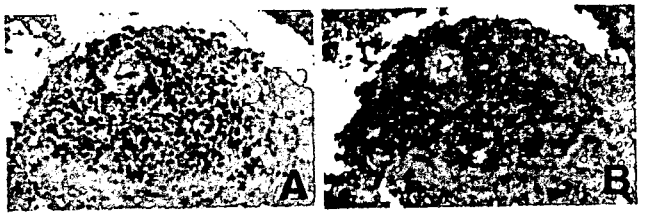

Fig. 2 Photomicrographs showing neoplastic cells in the perivascular area (A: hematoxylin and eosin stain, ×200) and positive immunostaining for anti-CD20 antibody (B: × 200).

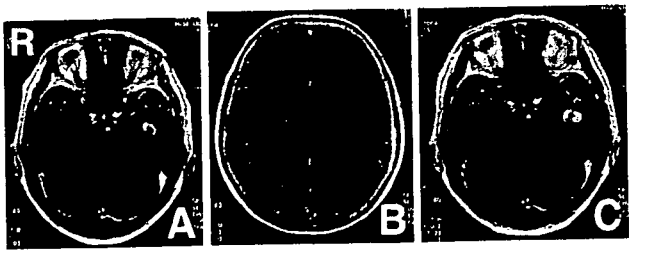

Fig. 3 T_1-weighted magnetic resonance images with contrast medium showing tumor shrinkage after two cycles of high-dose methotrexate therapy (A, B), and tumor enlargement after three cycles (C).

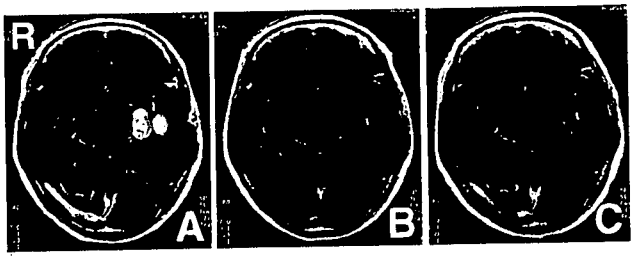

Fig. 4 T_1-weighted magnetic resonance images with contrast medium after four cycles of rituximab showing tumor enlargement (A), after three cycles of temozolomide showing complete disappearance of the tumor (B), and after 13 cycles of temozolomide showing no signs of tumor recurrence (C).

progressive mental deterioration and somnolence. MR imaging with contrast medium demonstrated enhanced lesions in the left temporal horn of the lateral ventricle, septum pellucidum, and periventricular area of the fourth ventricle (Fig. 1).

On admission, her Karnofsky performance status score was 30, and her Hasegawa dementia scale was 4/30. She underwent diagnostic MR imaging-guided biopsy. The histological diagnosis was B-cell lymphoma (Fig. 2). Computed tomography of the chest, abdomen, and pelvis revealed no evidence of systemic lymphoma. She had a medical history of diabetes mellitus, hypertension, and hypercholesteremia. Her renal function was adequate for systemic chemotherapy with high-dose MTX (creatinine clearance 80 ml/min), so she received three cycles of high-dose MTX (3.5 g/m^2) consisting of a 3-hour infusion on the 1st day of treatment and oral procarbazine (60 mg/m^2) on days 1–7. Urine alkalinization was started with sodium bicarbonate before the start of MTX infusion, and citrovorum-factor rescue was begun at 24 hours after. She manifested no clinical signs of toxicity except for nausea and appetite loss after each cycle. MR imaging after the second cycle revealed that the lesions had shrunk significantly (Fig. 3A, B). Her Karnofsky performance status score improved to 60 and Hasegawa dementia scale to 17/30. However, MR imaging after the third cycle revealed that the tumor in the left temporal lobe was enlarged (Fig. 3C).

Since adjuvant whole-brain irradiation after high-dose MTX can result in delayed neurotoxicity in the elderly, we administered four cycles of induction rituximab (375 mg/m^2/week for 4 consecutive weeks). The infusion was started at 50 mg/hr and gradually increased to 200 mg/hr. She showed no signs of toxicity, new neurological deficits, or mental deterioration. However, MR imaging after completion of the fourth cycle revealed enlargement of the tumor in the left temporal lobe (Fig. 4A). Therefore, a third line of treatment consisting of three cycles of oral temozolomide (150 mg/m^2/day for 5 days) was implemented at intervals of 28 days. Administration of temozolomide for patients with primary CNS lymphoma was approved by the Institutional Review Board in our hospital. Minor responses were observed after the first and second cycles of the treatment. The enhanced lesion disap-

peared completely after the third cycle (Fig. 4B). Temozolomide treatment was continued at the same dosage for a total of 16 cycles. There were no episodes of toxicity including leukopenia or thrombocytopenia. She now requires only limited medical support in daily life with Karnofsky performance status score of 40, and there has been no recurrence for more than 1 year (Fig. 4C).

Discussion

Elderly patients represent an important subgroup that accounts for approximately half of all primary CNS lymphoma cases, but only radiotherapy has produced disappointing results.[19] High-dose MTX-based chemotherapy regimens combined with whole-brain radiotherapy has achieved improved clinical outcomes, but as many as 80% of elderly patients suffered delayed neurotoxicity.[1] Therefore, high-dose MTX and procarbazine were selected as the initial treatment in the present patient. However, tumor enlargement was noted after the third cycle. About half of immunocompetent patients with primary CNS lymphoma who achieve complete recovery after primary treatment suffer relapse, and the disease is refractory in 10–15%.[7,9] The prognosis for both recurrent and progressive primary CNS lymphoma is poor and most patients die within 2–4 months of neurological deterioration.[7,21]

The present patient underwent further chemotherapy with rituximab and temozolomide. Rituximab is a chimeric monoclonal antibody against the CD20 antigen commonly found in B-cell non-Hodgkin's lymphoma. The mechanisms of action include complement-mediated cytotoxicity, antibody-mediated phagocytosis, and antibody-dependent growth inhibition and apoptosis.[15] Rituximab is effective against relapsed B-cell non-Hodgkin's lymphoma,[14,18] but the potential efficacy is limited by its high molecular weight, which prevents transport across the intact blood-brain barrier. Rituximab may sensitize CD20-positive B lymphoma cells to cytotoxic chemotherapy by down-regulating interleukin-10 and Bcl-2 via inactivation of the signal transducer and activator of transcription 3 protein.[3,4] Therefore, treatment with rituximab followed by an alkylating agent such as temozolomide may offer synergistic lymphoma cell killing without overlapping toxicities. Such combination treatment was given to seven patients, of whom five patients achieved radiographic complete response and two patients had partial response.[26]

Temozolomide does not exhibit the cumulative myelotoxicity associated with similar alkylating agents such as lomustine and procarbazine in the PCV regimen (procarbazine, lomustine, and vincristine) which is effective against recurrent primary CNS lymphoma.[11] In addition, temozolomide is bioavailable to the CNS, as one-third of orally administered temozolomide was detected in the cerebrospinal fluid of patients with malignant brain tumors.[16] Temozolomide has been used successfully as first-line chemotherapy in two cases of primary CNS lymphoma,[12,13] including a 72-year-old patient with impaired renal function.[13] After two cycles of treatment, complete response was obtained. However, the patient developed pneumonia and expired during treatment. The etiology of pneumonia was unclear. Moreover, temozolomide yielded objective responses as salvage therapy for patients with primary CNS lymphoma.[23] A 65-year-old patient was initially treated with high-dose MTX-based treatment.[23] However, the treatment was terminated because of renal toxicity and congestive heart failure. The patient was referred to radiotherapy followed by four courses of chemotherapy. Although complete response was achieved, recurrence of the disease was found 3 months later. The patient was treated with four courses of temozolomide. A complete response was achieved after the second course without any grade 3–4 toxicity. Temozolomide exhibits single-agent activity against primary CNS lymphoma and even patients with treatment failure can tolerate temozolomide therapy without major toxicity.[25] Twenty-three patients who failed to respond to treatment including high-dose MTX and/or radiation therapy were enrolled.[25] Median age was 60 years (range 18 to 75 years). There were five complete remissions and one partial response for an objective response rate of 26%. There was no hematological grade 3–4 toxicity. One patient developed grade 3 vomiting. Grade 1–2 toxicity mainly consisted of nausea (15%), vomiting (6%), fatigue (9%), and neurological symptoms (9%).

The present elderly woman with relapse of primary CNS lymphoma manifested complete radiographic response to three cycles of oral temozolomide chemotherapy without experiencing toxicity. We suggest that temozolomide is a promising new agent for the treatment of relapsed primary CNS lymphoma.

References

1) Abrey LE, DeAngelis LM, Yahalom J: Long-term survival in primary CNS lymphoma. *J Clin Oncol* 16: 859–863, 1998
2) Abrey LE, Yahalom J, DeAngelis LM: Treatment for primary CNS lymphoma: the next step. *J Clin Oncol* 18: 3144–3150, 2000

3) Alas S, Bonavida B: Rituximab inactivates signal transducer and activation of transcription 3 (STAT3) activity in B-non-Hodgkin's lymphoma through inhibition of the interleukin 10 autocrine/paracrine loop and results in down-regulation of Bcl-2 and sensitization to cytotoxic drugs. *Cancer Res* 61: 5137-5144, 2001
4) Alas S, Emmanouilides C, Bonavida B: Inhibition of interleukin 10 by rituximab results in down-regulation of bcl-2 and sensitization of B-cell non-Hodgkin's lymphoma to apoptosis. *Clin Cancer Res* 7: 709-723, 2001
5) Batchelor T, Carson K, O'Neill A, Grossman SA, Alavi J, New P, Hochberg F, Priet R: Treatment of primary CNS lymphoma with methotrexate and deferred radiotherapy: a report of NABTT 96-07. *J Clin Oncol* 21: 1044-1049, 2003
6) DeAngelis LM: Primary CNS lymphoma: treatment with combined chemotherapy and radiotherapy. *J Neurooncol* 43: 249-257, 1999
7) DeAngelis LM, Yahalom J, Thaler HT, Kher U: Combined modality therapy for primary CNS lymphoma. *J Clin Oncol* 10: 635-643, 1992
8) Ferreri AJ, Reni M, Villa E: Therapeutic management of primary central nervous system lymphoma: lessons from prospective trials. *Ann Oncol* 11: 927-937, 2000
9) Glass J, Shustik C, Hochberg FH, Cher L, Gruber ML: Therapy of primary central nervous system lymphoma with pre-irradiation methotrexate, cyclophosphamide, doxorubicin, vincristine, and dexamethasone (MCHOD). *J Neurooncol* 30: 257-265, 1996
10) Guha-Thakurta N, Damek D, Pollack C, Hochberg FH: Intravenous methotrexate as initial treatment for primary central nervous system lymphoma: response to therapy and quality of life of patients. *J Neurooncol* 43: 259-268, 1999
11) Herrlinger U, Brugger W, Bamberg M, Kuker W, Dichgans J, Weller M: PCV salvage chemotherapy for recurrent primary CNS lymphoma. *Neurology* 54: 1707-1708, 2000
12) Herrlinger U, Kuker W, Platten M, Dichgans J, Weller M: First-line therapy with temozolomide induces regression of primary CNS lymphoma. *Neurology* 58: 1573-1574, 2002
13) Lerro KA, Lacy J: Case report: a patient with primary CNS lymphoma treated with temozolomide to complete response. *J Neurooncol* 59: 165-168, 2002
14) Maloney DG, Grillo-Lopez AJ, Bodkin DJ, White CA, Liles TM, Royston I, Varns C, Rosenberg J, Levy R: IDEC-C2B8: results of a phase I multiple-dose trial in patients with relapsed non-Hodgkin's lymphoma. *J Clin Oncol* 15: 3266-3274, 1997
15) Maloney DG, Smith B, Rose A: Rituximab: mechanism of action and resistance. *Semin Oncol* 29: 2-9, 2002
16) Marzolini C, Decosterd LA, Shen F, Gander M, Leyvraz S, Bauer J, Buclin T, Biollaz J, Lejeune F: Pharmacokinetics of temozolomide in association with fotemustine in malignant melanoma and malignant glioma patients: comparison of oral, intravenous, and hepatic intra-arterial administration. *Cancer Chemother Pharmacol* 42: 433-440, 1998
17) McAllister LD, Doolittle ND, Guastadisegni PE, Kraemer DF, Lacy CA, Crossen JR, Neuwelt EA: Cognitive outcomes and long-term follow-up results after enhanced chemotherapy delivery for primary central nervous system lymphoma. *Neurosurgery* 46: 51-61, 2000
18) McLaughlin P, Grillo-Lopez AJ, Link BK, Levy R, Czuczman MS, Williams ME, Heyman MR, Bence-Bruckler I, White CA, Cabanillas F, Jain V, Ho AD, Lister J, Wey K, Shen D, Dallaire BK: Rituximab chimeric anti-CD20 monoclonal antibody therapy for relapsed indolent lymphoma: half of patients respond to a four-dose treatment program. *J Clin Oncol* 16: 2825-2833, 1998
19) Nelson DF, Martz KL, Bonner H, Nelson JS, Newall J, Kerman HD, Thomson JW, Murray KJ: Non-Hodgkin's lymphoma of the brain: can high dose, large volume radiation therapy improve survival? Report on a prospective trial by the Radiation Therapy Oncology Group (RTOG): RTOG 8315. *Int J Radiat Oncol Biol Phys* 23: 9-17, 1992
20) Plotkin SR, Batchelor TT: Advances in the therapy of primary central nervous system lymphoma. *Clin Lymphoma* 1: 263-277, 2001
21) Pollack IF, Lunsford LD, Flickinger JC, Dameshek HL: Prognostic factors in the diagnosis and treatment of primary central nervous system lymphoma. *Cancer* 63: 939-947, 1989
22) Reni M, Ferreri AJ: Therapeutic management of refractory or relapsed primary central nervous system lymphomas. *Ann Hematol* 80 Suppl 3: B113-117, 2001
23) Reni M, Ferreri AJ, Landoni C, Villa E: Salvage therapy with temozolomide in an immunocompetent patient with primary brain lymphoma. *J Natl Cancer Inst* 92: 575-576, 2000
24) Reni M, Ferreri AJ, Villa E: Second-line treatment for primary central nervous system lymphoma. *Br J Cancer* 79: 530-534, 1999
25) Reni M, Mason W, Zaja F, Perry J, Franceschi E, Bernardi D, Dell'Oro S, Stelitano C, Candela M, Abbadessa A, Pace A, Bordonaro R, Latte G, Villa E, Ferreri AJ: Salvage chemotherapy with temozolomide in primary CNS lymphomas: preliminary results of a phase II trial. *Eur J Cancer* 40: 1682-1688, 2004
26) Wong ET, Tishler R, Barron L, Wu JK: Immunochemotherapy with rituximab and temozolomide for central nervous system lymphomas. *Cancer* 101: 139-145, 2004

Address reprint requests to: Keishi Makino, M.D., Department of Neurosurgery, Kumamoto University Graduate School, 1-1-1 Honjo, Kumamoto 860-8556, Japan.
e-mail: kmakino@fc.kuh.kumamoto-u.ac.jp

EXPRESSIVE AND RECEPTIVE LANGUAGE AREAS DETERMINED BY A NON-INVASIVE RELIABLE METHOD USING FUNCTIONAL MAGNETIC RESONANCE IMAGING AND MAGNETOENCEPHALOGRAPHY

Kyousuke Kamada, M.D., Ph.D.
Department of Neurosurgery,
The University of Tokyo,
Tokyo, Japan

Yutaka Sawamura, M.D., Ph.D.
Department of Neurosurgery,
Hokkaido University,
Sapporo, Japan

Fumiya Takeuchi, Ph.D.
Research Institute for Electric Science,
Hokkaido University,
Sapporo, Japan

Shinya Kuriki, Ph.D.
Research Institute for Electronic Science,
Hokkaido University,
Sapporo, Japan

Kensuke Kawai, M.D., Ph.D.
Department of Neurosurgery,
The University of Tokyo,
Tokyo, Japan

Akio Morita, M.D., Ph.D.
Department of Neurosurgery,
The University of Tokyo,
Tokyo, Japan

Tomoki Todo, M.D., Ph.D.
Department of Neurosurgery,
The University of Tokyo,
Tokyo, Japan

Reprint requests:
Kyousuke Kamada, M.D., Ph.D., and
Tomoki Todo, M.D., Ph.D.,
Department of Neurosurgery,
The University of Tokyo,
7-3-1 Hongo, Bunkyo-ku,
Tokyo 113-8655 Japan.
Email: kamady-k@umin.ac.jp

Received, March 23, 2006.
Accepted, October 13, 2006.

OBJECTIVE: It is known that functional magnetic resonance imaging (fMRI) and magnetoencephalography (MEG) are sensitive to the frontal and temporal language function, respectively. Therefore, we established combined use of fMRI and MEG to make reliable identification of the global language dominance in pathological brain conditions.

METHODS: We investigated 117 patients with brain lesions whose language dominance was successfully confirmed by the Wada test. All patients were asked to generate verbs related to acoustically presented nouns (verb generation) for fMRI and to read three-letter words for fMRI and MEG.

RESULTS: fMRI typically showed prominent activations in the inferior and middle frontal gyri, whereas calculated dipoles on MEG typically clustered in the superior temporal region and the fusiform gyrus of the dominant hemisphere. A total of 87 patients were further analyzed using useful data from both the combined method and the Wada test. Remarkably, we observed a 100% match of the combined method results with the results of the Wada test, including two patients who showed expressive and receptive language areas dissociated into bilateral hemispheres.

CONCLUSION: The results demonstrate that this non-invasive and repeatable method is not only highly reliable in determining language dominance, but can also locate the expressive and receptive language areas separately. The method may be a potent alternative to invasive procedures of the Wada test and useful in treating patients with brain lesions.

KEY WORDS: Expressive language function, Functional magnetic resonance imaging, Language dominance, Magnetoencephalography, Receptive language function

Neurosurgery 60:296–306, 2007 DOI: 10.1227/01.NEU.0000249262.03451.0E www.neurosurgery-online.com

Brain asymmetries have been of considerable interest in neurology for more than a century. Based on clinicopathological studies, the "classical mode" of language organization consists of a frontal "expressive" area for planning and executing speech and writing, and a temporal "receptive" area for analysis and identification of linguistic sensory stimuli. This basic scheme of language functions has generally been accepted, with the assumption that both expressive and receptive functions dominantly exist in the same hemispheric side.

The Wada test has been considered the most reliable method to determine language dominance. According to one of the largest studies performed to date, 4 and 96% of right-handed subjects with chronic epilepsy have speech dominance in the right and left hemispheres, respectively (3). Furthermore, several studies suggested the possibility of atypical language representation in patients with chronic epilepsy (20–30%) (9, 28). However, the procedure of successive anesthetization of each hemisphere by intracarotid injections of sodium amobarbital requires catheterization and irradiation. Furthermore, the Wada test results can only demonstrate a relative distribution of language functions across the two hemispheres. More detailed information on localization of specified language functions within a hemisphere is important for understanding the language networks, as well as the treatment of brain lesions.

The use of functional magnetic resonance imaging (fMRI) has recently been developed to identify the hemisphere with language dominance. Most language fMRI studies have observed activations in the inferior frontal gyrus (IFG) and middle frontal gyrus (MFG) using tasks such as word generation and categorization (16, 24, 29). Detection of the receptive language area by fMRI has been reported to be more difficult than that of the expressive language function, and the use of listening or sentence comprehension tasks has resulted in visualization of only a few pixels in the temporoparietal region (8, 16, 25, 26). In addition, a fundamental limitation of an fMRI-based brain mapping is the varying degrees of regional hemodynamic responses under pathological brain conditions (7, 10, 15). Therefore, a clinical interpretation of localized activations on fMRI remains complicated and controversial.

Magnetoencephalography (MEG) reflects intracellular electric current flow in the brain and allows accurate localization of the current dipole sources. Dipoles of MEG deflections that peaked at approximately 400 milliseconds after word presentation (late responses) have been observed to localize in the temporoparietal regions. These late responses have been considered to be related to the receptive language function (19, 20). We have also observed dense dipole clusters of the semantic late responses in the superior temporal gyrus (STG), supramarginal gyrus (SmG), and fusiform gyrus (FuG) of the suspected dominant hemisphere (11, 12). Therefore, we sought to use MEG not only as an additional diagnostic tool for identifying the language dominance, but also to localize the receptive language center.

In the present study, we describe a non-invasive method to locate the expressive and receptive language areas by co-utilizing fMRI and MEG. The language dominance determined by our method matched the results from the Wada test with 100% accuracy. The usefulness of the method was well demonstrated, especially in those patients who showed dissociated expressive and receptive language functions. The data show that this method is highly reliable and may be useful in the management of patients with brain lesions as well as in studying normal brain functions.

METHODS

Patients

The functional brain mapping using fMRI (with the verb generation task) and MEG was performed in 117 patients with brain lesions since August 1999 (>7 yr) after this project was approved by the Institutional Committee for Ethics (*Table 1*). fMRI studies with the abstract/concrete (A/C) categorization task were also performed in 106 patients. Ninety-seven patients also underwent the Wada test to confirm the dominant cerebral hemisphere for language functions. Six patients showed negative Wada test results owing to the steal effect of a large arteriovenous malformation (AVM) or an overdose. The final analyses were performed in 87 patients (48 men, 39 women), who underwent Wada test, fMRI, and MEG investigations. The mean age (± standard deviation) was 43.6 ± 14.1 years. The Edinburgh Handedness Inventory was used to estimate the patients' handedness (18). A written informed consent was obtained from the patient or his/her family before participation in the study.

Magnetic Resonance Protocols

Anatomic magnetic resonance imaging (MRI) and fMRI were performed during the same session with a 1.5-T whole-body magnetic resonance scanner with echo-planar capabilities and a standard whole-head transmit-receiver coil (Siemens Vision, Erlangen, Germany). During the procedures, foam cushions were used to immobilize the head.

Language fMRI

The patients were instructed to respond to all language tasks silently. fMRI data was acquired with a T2-weighted echo-planar imaging sequence (echo time, 62 ms; repetition time, 114 ms; flip angle, 90 degrees; slice thickness, 4 mm; slice gap, 2 mm; field of view, 260 mm; matrix, 64 × 128; 14 slices). Each fMRI session consisted of three dummy scan volumes followed by three activation and four baseline (rest) periods. During each period, five echo-planar imaging volumes were collected, yielding a total of 38 imaging volumes and 2 minutes 32 seconds in measurement time for each session. fMRI data of language-related semantic responses were acquired as follows. All subjects were examined with two different lexical semantic language paradigms; verb generation by listening to nouns and A/C categorization by reading words. All words for semantic tasks were selected from common Japanese words listed in the electronic dictionary of the National Institute for Japanese Language.

Verb Generation Task

For the auditory stimuli (duration ranges were between 400 and 600 ms), common concrete nouns spoken by a native Japanese speaker with a flat intonation were recorded and digitized with a sampling rate of 44,000 Hz. A backward playback of the sound files (reference sounds) was used to eliminate the primary auditory activation during the rest periods with the same inter-stimuli intervals (1600–2400 ms) as the active periods. The auditory stimuli were delivered binaurally via two 5-m-long plastic tubes terminating at a headphone. The sound intensity was approximately 95 dB sound pressure level at the subject's ear. Subjects were instructed to silently generate a verb related to each presented noun during the active periods and passively listen to the reference sounds during the rest periods.

A/C Categorization Task

Visual stimuli were presented on a liquid crystal display monitor with a mirror above the head coil allowing the patients to see the stimuli. Words consisting of three *Kana* letters (Japanese phonetic symbols) were presented in a 300-millisecond exposure time with interstimuli intervals ranging from 2800 to 3200 milliseconds. Patients were instructed to categorize the presented word silently into "abstract" or "concrete" based on the

TABLE 1. Summary of patients' brain lesions types[a]

	Glioma	Chronic Epilepsy	AVM	Meningioma	Cavernous malformation	Cerebral ischemia	Total
fMRI with VG + MEG	44	39	18	6	4	6	117
fMRI with A/C	41	34	15	6	4	6	106
Amytal test	42	29	16	6	4	0	97
Final analyses	39	26	12	6	4	0	87

[a] AVM, arteriovenous malformation; fMRI, functional magnetic resonance imaging; VG, verb generation task; MEG, magnetoencephalography; A/C, abstract/concrete categorization task.

nature of the word. During interval periods, patients passively viewed random dots of destructured *Kana* letters that were controlled to have the same luminance as the stimuli to eliminate primary visual responses.

Before scanning, all patients had a brief practice time, and the fMRI examinations were repeated for each task to confirm the reproducibility. After data acquisition, a motion detection program (MEDx; Medical Numerics, Sterling, VA) discarded fMRI sessions containing motion artifacts exceeding 25% of the pixel size. A Gaussian spatial filter (6 mm in half width) was applied, and functional activation maps were calculated by estimating the Z-scores between the rest and activation periods using Dr. View (Asahi Kasei, Tokyo, Japan). Pixels with Z-scores higher than 2.2 ($P < 0.05$) were considered to indicate real activation and were used for mapping. Image distortion of fMRI was corrected by maximizing the mutual information of the fMRI data sets and three-dimensional T1-weighted MRI (3D-MRI) scans of the patient's brain (morphing compensation). The result from each fMRI session was co-registered with the 3D-MRI by the Affine transformation (5). After total number of the activated pixels in the IFG and MEG were automatically counted, a patient was considered to have unilateral language dominance when hemispheric pixels of one hemisphere counted less than 70% of the other hemisphere. Otherwise, the language dominance was considered bilateral.

Language MEG

The MEG signals were recorded with a 204-channel biomagnetometer (VectorView; Neuromag, Helsinki, Finland) in a magnetically shielded room. To confirm the reproducibility, we acquired two data sets for each task by repeating the MEG recording on two different days. One hundred fifty nouns consisting of three *Kana* letters were visually presented with a 300-millisecond exposure time with interstimuli intervals ranging from 2800 to 3200 milliseconds. Patients were instructed to judge whether or not the presented word was "abstract" or "concrete" based on the nature of the word and to push a button with the index or middle finger (*Kana* reading task). Each epoch consisted of a 500-millisecond prestimulus baseline and a stimulus followed by a 1500-millisecond analysis period. Epochs with a reaction time exceeding 1200 milliseconds and MEG examinations with a successful task performance less than 70% were discarded.

One hundred fifty epochs of the magnetic signals were averaged and digitally filtered between 0.1 to 30 Hz. Significant MEG deflections were visually identified based on the square root mean fields of more than 10 sensors in the frontotemporal (FT) or temporo-occipital (TO) regions. Locations and dipole moments of equivalent current dipoles were calculated every 2 milliseconds from 250 to 600 milliseconds after the stimulus onsets using the single equivalent dipole and sphere head models. Only those dipoles of which the measured and the calculated field distributions showed a correlation value of more than 0.85 and confidence volumes less than 1000 mm^3 were used. To confirm the calculated results, the same MEG time sections were analyzed using a current density map (low-resolution tomography; LORETA, Curry, Neuroscan, and Compumedics USA, El Paso, TX). The coordinates of the MEG system were transformed into anatomic 3D-MRI scans by identifying external anatomic fiduciary markers (nasion, left/right preauricular points), and estimated dipoles were superimposed onto the 3D-MRI scans.

Dipoles located in the temporal region, including the STG, MTG, SmG, and FuG, were manually counted. A patient was considered to have unilateral language dominance when hemispheric dipoles of one hemisphere counted less than 70% of the other hemisphere. Otherwise, the language dominance was considered bilateral.

Determination of Language Dominance using fMRI and MEG

On the basis of the results of language fMRI and MEG, we determined language dominance for each patient. When the semantic activation in one side of the IFG and MFG was wider than that of the other side during the language fMRI tasks, a patient was considered to have unilateral dominance for the expressive language function. When one side of the temporal region included more MEG dipoles than the other during the language MEG task, we determined that a patient had laterality of the receptive language function.

The Wada Test

All patients received injections of amobarbital (100 mg in a 10% solution, Amytal; Eli Lilly and Co., Indianapolis, IN) through a catheter placed in the internal carotid artery. Language testing was performed during the observation period of maximal amobarbital action as indicated by contralateral